

Measuring the Josephson plasma resonance in $\text{Bi}_2\text{Sr}_2\text{CaCu}_2\text{O}_8$ using intense coherent THz synchrotron radiation

E. J. Singley,^{1,*} M. Abo-Bakr,² D. N. Basov,³ J. Feikes,² P. Guptasarma,⁴ K. Holldack,² H. W. Hübers,⁵ P. Kuske,² Michael C. Martin,^{1,†} W. B. Peatman,² U. Schade,² and G. Wüstefeld²

¹*Advanced Light Source Division, Lawrence Berkeley National Laboratory, 1 Cyclotron Road, Berkeley, California 94720, USA*

²*Berliner Elektronenspeicherring-Gesellschaft für Synchrotronstrahlung m.b.H., Albert-Einstein-Strasse 15, D-12489 Berlin, Germany*

³*Department of Physics, University of California, San Diego, 9500 Gilman Drive, La Jolla, California 92093, USA*

⁴*University of Wisconsin-Milwaukee, 1900 East Kenwood Boulevard, Milwaukee, Wisconsin 53211, USA*

⁵*Institut für Weltraumsensorik und Planetenerkundung, Rutherford-Strasse 2, D-12489 Berlin, Germany*

(Received 1 December 2003; published 30 March 2004)

Infrared (IR) spectroscopy has been employed to investigate the c axis reflectivity of $\text{Bi}_2\text{Sr}_2\text{CaCu}_2\text{O}_8$ in the sub-THz frequency region. In order to reach this challenging frequency range a synchrotron source has been employed. Working in a special low-momentum compaction mode of operation where the electron bunch shape is significantly shortened and distorted, stable broadband coherent (superradiant) very far-infrared radiation is produced with orders of magnitude more intensity than conventional thermal and synchrotron sources. Using this source for reflectivity measurements we have been able to observe the Josephson plasma resonance (JPR) in optimally doped $\text{Bi}_2\text{Sr}_2\text{CaCu}_2\text{O}_8$. Evidence is found for an inhomogeneous distribution of superfluid density within the sample. This source allows us to investigate charge dynamics in this extremely anisotropic superconductor, and opens up the possibility to study other highly correlated systems in this critical low-energy region.

DOI: 10.1103/PhysRevB.69.092512

PACS number(s): 74.72.-h, 07.57.Hm, 41.60.Ap, 74.81.-g

The terahertz (THz) and sub-THz region of the electromagnetic spectrum lies between the infrared and the microwave. This boundary region is beyond the normal reach of optical and electronic measurement techniques associated with these better-known neighbors. Only over the past decade has this THz region become scientifically available with moderate intensity broadband sources produced by ultrafast laser pulses incident on biased semiconductors or nonlinear crystals.^{1,2} Recently, a much higher power source of THz radiation was demonstrated: coherent synchrotron radiation (CSR).³ Besides offering high power, CSR enables broadband optical techniques to be extended to nearly the microwave region, and it inherently has subpicosecond pulses. As a result, new opportunities for scientific research and applications are enabled across a diverse array of disciplines: condensed matter physics, medicine, manufacturing, and space and defense industries. CSR will have a strong impact on THz imaging, spectroscopy, femtosecond dynamics, and driving novel nonlinear processes.⁴ Here we present the first CSR scientific experiment in which we take advantage of the ultralow-frequency radiation to make optical reflectivity measurements of the c -axis Josephson plasma resonance in the highly anisotropic, optimally doped high-temperature superconductor $\text{Bi}_2\text{Sr}_2\text{CaCu}_2\text{O}_8$.

CSR is emitted by bunches of accelerated charged particles when the bunch length is shorter than the wavelength being emitted. When this criterion is met, all the particles emit in phase, and a single-cycle electromagnetic pulse results with an intensity proportional to the square of the number of particles in the bunch.^{5,6} It is this quadratic dependence that can produce colossal intensities even with fairly low beam currents.³ Until recently CSR has not typically been observed in synchrotron storage rings because the electron bunch lengths are longer than the vacuum chamber

height, so full-bunch coherent emission is at wavelengths beyond the waveguide cutoff and is therefore suppressed. The first observations of CSR from storage rings were of quasichaotic bursts of intensity caused by density modulations in unstable electron bunches.⁷⁻¹⁰ While studies of this bursting phenomenon have provided glimpses into the powers available with CSR, the unstable nature of the emission makes this a problematic THz source for scientific measurements. Recently, stable CSR has been produced with a storage ring at the BESSY synchrotron facility.¹¹ This feat was achieved by shortening the electron bunches to a point where the CSR itself feeds back on other electrons in the bunch, causing a distortion of the longitudinal bunch profile to a non-Gaussian distribution.¹² This skewed distribution has higher Fourier components and therefore allows CSR production to higher frequencies than the nominal bunch length would allow.

Figure 1 shows a log-log plot of the measured intensity spectrum of the CSR produced at BESSY along with two other conventional sources used for infrared measurements. Below 20 cm^{-1} both the Hg arc lamp and Globar source decrease strongly, and are below our detection limit at $\sim 7\text{ cm}^{-1}$. It is worth noting that a typical transmission or reflectance measurement requires additional mirrors, windows, and the sample itself all of which attenuate the signal such that the practical cut-off frequency will be a factor of 2–3 times higher. In contrast to the conventional sources the CSR intensity increases below 20 cm^{-1} , and is nearly four orders of magnitude larger at 7 cm^{-1} . Even higher intensities may be obtained while still remaining below the bursting instability threshold¹⁰ by tuning the electron bunch profile¹¹ and optimizing the spectrometer optics for longer wavelengths. The current profile was chosen such that the signal

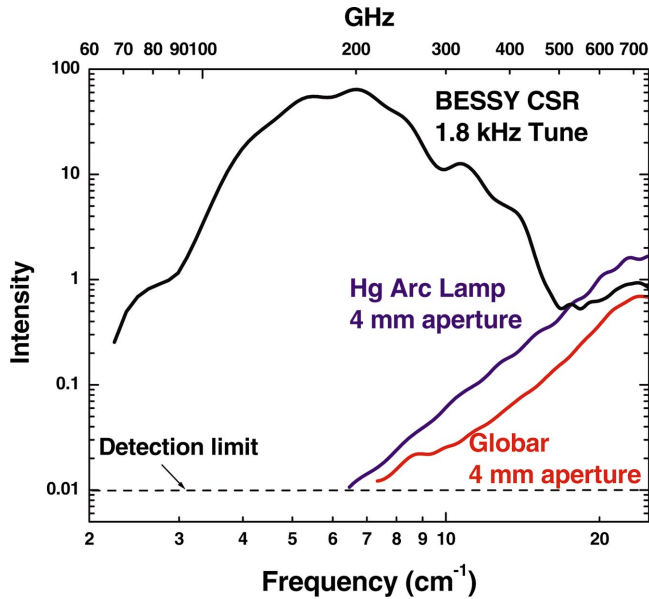


FIG. 1. (Color) Measured far-IR intensity for the BESSY CSR source, compared to conventional Hg arc lamp and Globar sources. These intensity measurements were performed with an open sample path in the Bruker 66v/S FTIR interferometer, a $6 \mu\text{m}$ Mylar beam splitter, and the 1.6 K Si bolometer detector. While the turn-on of the CSR source below 20 cm^{-1} is a real effect of the CSR emission process, the drop-off at the low-frequency end is due to a combination of diffraction losses in the optical path of the beamline and the cut-offs of the optical components, such as the Mylar beam splitter in the interferometer.

to noise of the sample in reflectance mode was within $\pm 2\%$ at 7 cm^{-1} . The decrease in the CSR signal below 5 cm^{-1} is most likely not intrinsic to the source, rather due to optical elements in the beamline/spectrometer, the response of the detector, and/or diffraction cutoff of the beamline collection optics.

Using the broad, high power, sub-THz spectrum shown in Fig. 1, we have been able to extend traditional infrared reflectivity measurements on the high- T_c cuprate superconductor $\text{Bi}_2\text{Sr}_2\text{CaCu}_2\text{O}_8$ down to lower frequencies than previously possible. When the electric field is polarized parallel to the c axis, we clearly observe the development of a sub-THz plasma edge in the reflectance at $T < T_c$. The origin of the c -axis charge transport in the superconducting state is Josephson tunneling of Cooper pairs.¹³ The crystal structure provides a microscopic superconducting-insulating-superconducting junction. In the normal state charge transport between CuO_2 planes may be blocked by intermediate insulating Bi-O layers. However, in the superconducting state the Josephson effect allows for a charge current and hence three-dimensional (3D) superconductivity. The interpretation of Josephson tunneling as the source of the charge transport has been experimentally verified by observation of both DC and AC Josephson effect in $\text{Bi}_2\text{Sr}_2\text{CaCu}_2\text{O}_8$.¹⁴ The minimum observed in the reflectance at $T < T_c$ is the screened Josephson plasma frequency and holds important information about the rigidity of the superconducting state along the c axis.

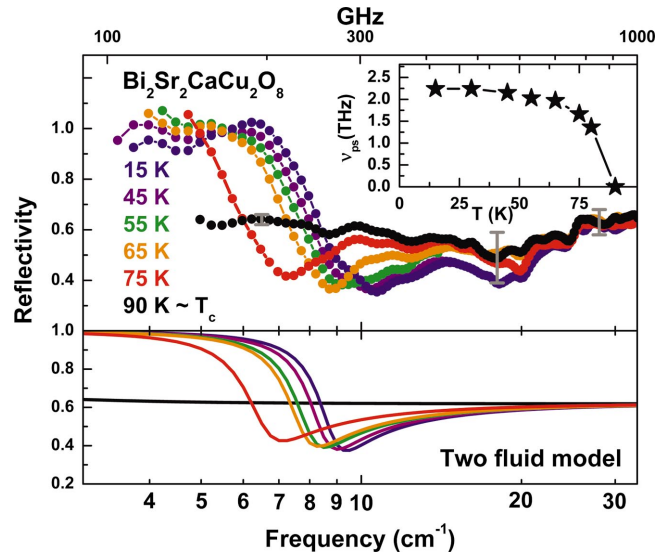


FIG. 2. (Color) Measured c -axis polarized near-normal reflectivity of $\text{Bi}_2\text{Sr}_2\text{CaCu}_2\text{O}_8$ (upper panel) for various representative temperatures at or below the superconducting transition temperature, T_c . A resonance that shifts with temperature and disappears above T_c is clearly observed. The lower panel shows the calculated reflectivity of a superconductor with a shifting Josephson plasma resonance. The inset of the top panel shows the temperature dependence of the unscreened superfluid plasma frequency as determined from fits to the data.

The energy scale of the Josephson plasma edge is directly related to the degree of anisotropy of the material. In nearly all families of high-temperature superconductors the plasma resonance has been observed with reflectance measurements in the far-infrared frequency range.¹⁵ The most notable exception is in the extremely anisotropic $\text{Bi}_2\text{Sr}_2\text{CaCu}_2\text{O}_8$ where at optimal doping the plasma edge has not been detected. By overdoping this compound (with Pb), and hence lowering the anisotropy (and T_c), a plasma edge in the reflectance has been seen near 40 cm^{-1} .¹⁶ Additionally, in the underdoped compounds a resonance is observed in magneto-absorption experiments in the microwave region, usually attributed to oscillations of the Josephson plasma.^{17,18} In optimally doped samples, sphere resonance experiments found no evidence of a resonance down to 7.5 cm^{-1} ,¹⁹ while time domain THz transmission measurements of a thin film have seen a resonance in the range of $7\text{--}12 \text{ cm}^{-1}$.²⁰ However, analysis of the latter feature was complicated due to the unconventional optical setup. In the present experiment reflectivity measurements on optimally doped $\text{Bi}_2\text{Sr}_2\text{CaCu}_2\text{O}_8$ ($T_c = 90 \text{ K}$) down to 4 cm^{-1} show the clear development of a plasma edge at $T < T_c$ attributed to the Josephson plasma resonance. An analysis of the reflectivity spectrum yields an unscreened plasma frequency of 74 cm^{-1} , and hence a c -axis penetration depth $\lambda_c = 21 \mu\text{m}$. Additional evidence is found for an inhomogeneous distribution of superfluid density within the sample.

Specular reflectance in the sub-THz region can be complicated if the wavelength of the probing radiation ($\sim 1 \text{ mm}$) approaches the sample size. Since achieving a single crystal of high-temperature superconductors with

c -axis dimension $\gg 1$ mm is difficult, a single crystal with large ab face was broken and assembled into a mosaic with a net c -axis length of ~ 8 mm. While this circumvents problems of diffraction effects, additional complications arise due to reflection from the epoxy that binds the individual crystals together. To account for this contribution to the measured reflectance the area of epoxy showing was estimated and the experimental reflectance was corrected accordingly. Measurements were performed with a Bruker 66v/S vacuum Fourier transform spectrometer, a 6 μm mylar beam splitter, and an IR Laboratories Si bolometer detector operating at 1.6 K and outfitted with a 5 mm diameter exit aperture Winston cone. The radiation source was a special low-alpha bunch compression mode of the BESSY storage ring¹¹ with a rms bunch length of 1.3 mm and between 10 and 20 mA of beam current evenly distributed over all RF buckets. Every sample measurement was interspersed with open reference channel measurements to account for any changes in the CSR source properties. Absolute values of the reflectivity were obtained by coating the sample *in situ* with a thin layer of gold, and using the gold-coated sample as a reference.

The top panel of Fig. 2 shows the experimental reflectivity in the sub-THz region on a logarithmic frequency scale. It is useful to examine the normal state spectrum at 90 K (black curve) to discuss the signal to noise in different frequency regions. On the high-energy side of the spectrum the signal to noise is $\pm 5\%$. This is due to the relatively low intensity of the source at these energies (see Fig. 1). The largest noise is in a small band near 20 cm^{-1} , where the uncertainty is $\pm 10\%$. This arises from 50 Hz electrical noise coupling to the stored electron beam and/or the beamline. The Fourier transform interferometer modulates this to the frequency range near 20 cm^{-1} . Most significant is the relatively small error of better than $\pm 2\%$ in the very low frequency range.²¹ Hence, the best response of the CSR measurement is the most inaccessible region for traditional infrared sources.

In contrast to the nearly flat and featureless spectrum at $T = T_c$, the $R(\omega)$ spectra at $T < T_c$ shows a strong ω dependence. Below T_c the spectrum has a shallow minimum followed by a strong rise in the reflectivity. At the lowest frequency the spectra saturate to a constant value near unity. As the temperature decreases in the superconducting state, both the minimum and reflectance edge increase in frequency, although this shift is nearly saturated by 15 K. The reflectance edge in the superconducting state signals the flow of supercurrents along the c axis. As the density of superfluid increases as the temperature is lowered, the reflectance edge shifts to higher frequencies. These strong changes in the reflectivity at $T < T_c$ are a result of the Josephson plasma resonance.

The minimum observed in the reflectivity corresponds to the screened plasma frequency of the superconducting carriers. The unscreened plasma frequency is given by $\nu_{ps} = \sqrt{\epsilon_\infty} \nu_{\text{min}}$ where ϵ_∞ corresponds to the dielectric constant which reproduces the constant reflectance at $T = T_c$. A minimal model that can account for the finite reflectivity at the plasma minimum and the rounding of the top of the plasma edge incorporates a second electronic component consisting of an over damped plasmon.²² In the bottom panel of Fig. 2

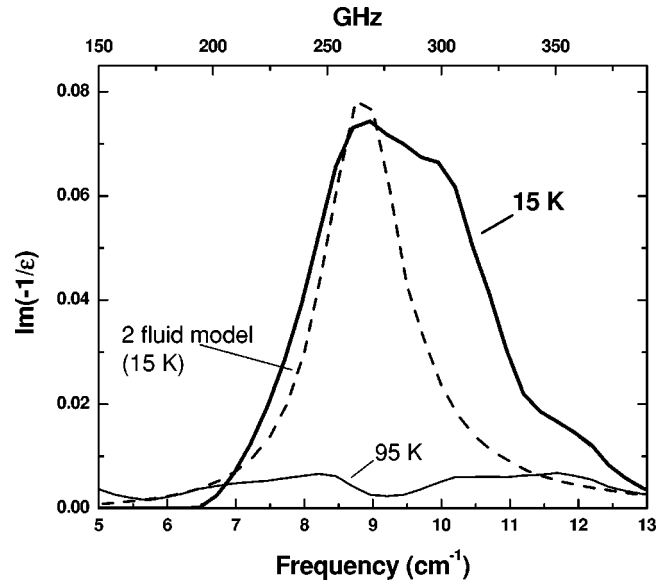


FIG. 3. Loss function $[-\text{Im}(1/\epsilon)]$ corresponding to the experimental reflectivity at 95 K (thin line) and 15 K (thick line). Also shown is the loss function for the two fluid model used to fit the 15 K reflectance (dashed line). The 95 K data are low and relatively featureless, giving an estimate for the influence of noise in the reflectance data. While both the model and data at 15 K show a strong absorption peaked just below 9 cm^{-1} critical differences exist. The model has the expected Lorentzian lineshape but the experimental data are asymmetric and much broader. This asymmetric broadening may be a signature for a distribution in the strength of the superfluid density throughout the sample.

the reflectivity of the sample is calculated using this two-fluid model. The magnitude and both the frequency and temperature dependence of the data in the top panel are well accounted for.

Using the above model to fit the data we are able to extract the value of the unscreened Josephson plasma frequency. At 15 K we obtain a value of $\nu_{ps} = 74\text{ cm}^{-1}$ (2.25 THz) which corresponds to a c -axis penetration depth value of $\lambda_c = 21\text{ }\mu\text{m}$. It is worth noting that the background reflectivity for this sample is anomalously high. This may in part be due to misalignment of the crystals in the mosaic which leads to a mixing of the a -axis and c -axis response. The result of this high background is an overestimation of ϵ_∞ . Using the location of the reflectance minimum in our raw data and a value of $\epsilon_\infty = 12$ obtained from a previous single crystal measurement²³ results in $\nu_{ps} = 35\text{ cm}^{-1}$ (1 THz) and $\lambda_c = 45\text{ }\mu\text{m}$. A similar value was obtained from $\sigma_2(\omega)$, generated from a Kramers-Kronig (KK) transformation of the $R(\omega)$ data. The complete temperature dependence of the Josephson plasma frequency is summarized in the inset of the top panel of Fig. 2. The plasma frequency rises quickly below T_c , and is nearly saturated at the low temperature limit by $T_c/2$.

These results are consistent with the doping dependence of λ_c . A smaller value of $\lambda_c = 12.6\text{ }\mu\text{m}$ has been obtained for overdoped $\text{Bi}_{1.6}\text{Pb}_{0.4}\text{Sr}_2\text{CaCu}_2\text{O}_8$, where the anisotropy is weaker and this value is therefore expected to be lower.²³ Likewise, microwave results of more anisotropic underdoped

$\text{Bi}_2\text{Sr}_2\text{CaCu}_2\text{O}_8$ reveal a correspondingly higher value of $\lambda_c \sim 110 \mu\text{m}$.¹⁸ As in nearly all cuprate families the superfluid density (and hence λ_c) changes most rapidly in the underdoped to optimally doped region, while smaller changes occur at higher doping levels.¹⁵

Further analysis of the frequency dependence of the JPR may yield information about properties of the superfluid within the CuO_2 planes.²⁴ Recent studies of the JPR for a series of $\text{La}_{2-x}\text{Sr}_x\text{CuO}_4$ crystals find a strong broadening of the minimum in $R(\omega)$ and corresponding asymmetry in the loss function for dopings where charge inhomogeneities are observed in the normal state.²⁵ These findings are accounted for by considering a distribution of superconducting plasma frequencies rather than the single value used in the two fluid model. In Fig. 3 we show the loss function calculated from the reflectance spectrum at 15 K for $\text{Bi}_2\text{Sr}_2\text{CaCu}_2\text{O}_8$. Also shown is the loss function calculated from the two fluid model used to fit the 15 K reflectance data. The model shows a Lorentzian lineshape. While the peak position of the data and model agree, the data have an asymmetric lineshape with much more weight at high frequencies. This breakdown of the two-fluid model is consistent with a distribution of superfluid density, rather than the single value used in the model. These findings are in line with reports of an inhomogeneous

electronic state in $\text{Bi}_2\text{Sr}_2\text{CaCu}_2\text{O}_8$.^{26,27} Future studies, especially on the doping dependence, may yield valuable information on the extent of these inhomogeneities and their impact on superconductivity.

The production of stable, high power, coherent synchrotron radiation at sub-terahertz frequencies opens a new region in the electromagnetic spectrum to explore physical properties of materials. Just as conventional synchrotron radiation has been a boon to x-ray science, coherent synchrotron radiation may lead to many new innovations and discoveries in terahertz science. We have demonstrated the ability to make absolute measurements of reflectivity with high photometric accuracy in this challenging sub-THz frequency range. As an initial test of the feasibility of using CSR in scientific applications, we have directly measured the Josephson plasma resonance in optimally doped $\text{Bi}_2\text{Sr}_2\text{CaCu}_2\text{O}_8$ for the first time. Our results bridge the gap between the microwave magnetoabsorption experiments and conventional far-infrared spectroscopy.

This work was supported by the Director, Office of Science, Office of Basic Energy Sciences, Division of Materials Sciences of the U. S. Department of Energy under Contract No. DE-AC03-76SF00098 and the Bundesministerium für Bildung und Forschung Grant 05 SR8KK19.

*Present address: Department of Physics, California State University, Hayward, CA 94542.

†Author to whom correspondence should be addressed. Email address: MCMartin@lbl.gov

¹D.H. Auston, K.P. Cheung, J.A. Valdmanis, and D.A. Kleinman, *Phys. Rev. Lett.* **53**, 1555 (1984).

²B. Ferguson and X.C. Zhang, *Nat. Mater.* **1**, 26 (2002).

³G.L. Carr, Michael C. Martin, Wayne R. McKinney, K. Jordan, George R. Neil, and G.P. Williams, *Nature (London)* **420**, 153 (2002).

⁴M. Sherwin, *Nature (London)* **420**, 131 (2002).

⁵J.S. Nodvick and D.S. Saxon, *Phys. Rev.* **96**, 180 (1954).

⁶C.J. Hirschmugl, M. Sagurton, and G.P. Williams, *Phys. Rev. A* **44**, 1316 (1991).

⁷A. Andersson, M.S. Johnson, and B. Nelander, *Opt. Eng. (Bellingham)* **39**, 3099 (2000).

⁸U. Arp, G.T. Fraser, A.R. Hight Walker, T.B. Lucatorto, K.K. Lehmann, K. Harkay, N. Sereno, and K.-J. Kim, *Phys. Rev. ST Accel. Beams* **4**, 054401 (2001).

⁹G.L. Carr, S.L. Kramer, J.B. Murphy, R.P.S.M. Lobo, and D.B. Tanner, *Nucl. Instrum. Methods Phys. Res. A* **463**, 387 (2001).

¹⁰J.M. Byrd, W.P. Leemans, A. Loftsdottir, B. Marcellis, Michael C. Martin, W.R. McKinney, F. Sannibale, T. Scarvie, and C. Steier, *Phys. Rev. Lett.* **89**, 224801 (2002).

¹¹M. Abo-Bakr, J. Feikes, K. Hollmack, and G. Wüstefeld, *Phys. Rev. Lett.* **88**, 254801 (2002).

¹²M. Abo-Bakr, J. Feikes, K. Hollmack, P. Kuske, W.B. Peatman, U. Schade, and G. Wüstefeld, *Phys. Rev. Lett.* **90**, 094801 (2003).

¹³D.N. Basov, T. Timusk, B. Dabrowski, and J.D. Jorgensen, *Phys. Rev. B* **50**, 3511 (1994).

¹⁴R. Kleiner and P. Müller, *Physica C* **293**, 156 (1997).

¹⁵S.V. Dordevic, E.J. Singley, D.N. Basov, S. Komiya, Y. Ando, E.

Bucher, C.C. Homes, and M. Strongin, *Phys. Rev. B* **65**, 134511 (2002).

¹⁶T. Motohashi, J. Shimoyama, K. Kitazawa, K. Kishio, K.M. Kojima, S. Uchida, and S. Tajima, *Phys. Rev. B* **61**, R9269 (2000).

¹⁷O.K.C. Tsui, N.P. Ong, Y. Matsuda, Y.F. Yan, and J.B. Peterson, *Phys. Rev. Lett.* **73**, 724 (1994).

¹⁸M.B. Gaifullin, Y. Matsuda, N. Chikumoto, J. Shimoyama, and K. Kishio, *Phys. Rev. Lett.* **84**, 2945 (2000); M.B. Gaifullin, Y. Matsuda, N. Chikumoto, J. Shimoyama, K. Kishio, and R. Yoshizaki, *ibid.* **83**, 3928 (1999).

¹⁹H. Shibata, *Phys. Rev. B* **59**, R11 672 (1999).

²⁰R. Mallozzi, J. Corson, J. Orenstein, J.N. Eckstein, and I. Bozovic, *J. Phys. Chem. Solids* **59**, 2095 (1998).

²¹The oscillations observed at low frequencies are not random, but rather a reproducible structure. A lack of phase resolution in the interferometer is the most likely source of this artificial structure.

²²The Drude model was used for the over damped plasmon with $\omega_p = 895 \text{ cm}^{-1}$ and $1/\tau = 8000 \text{ cm}^{-1}$.

²³S. Tajima, G.D. Gu, S. Miyamoto, A. Odagawa, and N. Koshizuka, *Phys. Rev. B* **48**, 16 164 (1993).

²⁴A.E. Koshelev, L.N. Bulaevskii, and M.P. Maley, *Phys. Rev. B* **62**, 14 403 (2000).

²⁵S.V. Dordevic, S. Komiya, Y. Ando, and D.N. Basov, *Phys. Rev. Lett.* **91**, 167401 (2003).

²⁶S.H. Pan, J.P. O'Neal, R.L. Badzey, C. Chamon, H. Ding, J.R. Engelbrecht, Z. Wang, H. Eisaki, S. Uchida, A.K. Gupta, K.-W. Ng, E.W. Hudson, K.M. Lang, and J.C. Davis, *Nature (London)* **413**, 282 (2001).

²⁷J. Corson, J. Orenstein, Seongshik Oh, J. O'Donnell, and J.N. Eckstein, *Phys. Rev. Lett.* **85**, 2569 (2000).